Δ_{33}-isobar contribution to the soft nucleon-nucleon potentials. II. $\pi\rho$-exchange potentials

Th. A. Rijken* and V. G. J. Stoks
Institute for Theoretical Physics, University of Nijmegen, Nijmegen, The Netherlands
(Received 19 December 1991)

Pion-rho-exchange nucleon-nucleon potentials are derived for one or two Δ isobars in the intermediate states. As in the companion work on two-pion exchange, strong dynamical pair suppression is assumed. At the $NN\pi,\rho$ and $N\Delta\pi,\rho$ vertices Gaussian form factors are incorporated into the relativistic two-body framework by using a dispersion representation for the π- and ρ-exchange amplitudes. The Fourier transformations are performed using factorization techniques for the energy denominators, taking into account the mass difference between the nucleon and the Δ isobar. The potentials are calculated in the adiabatic approximation of all planar and crossed three-dimensional momentum-space $\pi\rho$ diagrams. We also give the contributions of the $\pi\rho$ iteration, which can be subtracted or not, depending on whether one performs a coupled-channel calculation for, e.g., the NN, $N\Delta$ system, or a single NN-channel calculation.

PACS number(s): 13.75.Cs, 21.30.+y, 12.40.Qq

I. INTRODUCTION

In this second paper on the Δ_{33}-isobar contribution to the soft nucleon-nucleon potential, we derive the soft-core $\pi\rho$-exchange potentials due to one and two Δ_{33} isobars in the intermediate states. Our general approach to 2π-exchange potentials, and more generally to two-meson-exchange potentials, is given, in principle, in Ref. [1]. Starting from the relativistic two-body equations, we derive the two-meson-exchange potentials for the relativistic three-dimensional integral equation and for the Lippmann-Schwinger equation from the second-order Feynman diagrams. The channel space includes, in principle, the NN, the $N\Delta$, and the $\Delta\Delta$ channel. However, in working out the explicit potentials we restrict ourselves to the two-meson potentials in the NN sector only.

In the companion paper [2], we have extended the techniques described in Ref. [1] to cover mass differences of the baryons in the intermediate states. Using our techniques, in [2] we derived the 2π-exchange potentials with Δ isobars in the intermediate states. For the different important details of the derivations we refer the reader to the references given above. In particular, the important "factorization" technique involving two mesons with different masses will be used in the present paper for the π and the ρ meson. For earlier contributions to this field we refer to the work by the Stony Brook group [3] and by the Bonn group [4].

The reason for deriving, besides the 2π potentials, also the $\pi\rho$ potentials for isobars in the intermediate states is that (i) it is the only other sizable one of such contributions, and (ii) the $\pi\rho$ potentials tend to cancel the 2π potentials in the inner region [5]. This last feature could be important due to the singularities of the potentials near the origin. However, our soft-core potentials do not have these singularities. Still, it is known [6] that the 2π exchange from the Δ_{33}-isobar contribution is rather strong, so that all possible cancellation effects should be studied. In this respect, also the type of form factor could play an important role. Since in the case of two-meson exchange the volume integral of the potential is rather sensitive to the form factor, whereas for one-meson exchange it is not, the form factor can ameliorate the potentials considerably. This except for the long-range part, which is insensitive to the form factor. Maybe here the Gaussian form factor, which we use, has important advantages over the propagator type of form factors.

Another aspect is that one should be careful to avoid "double counting." Because the Δ_{33} isobar can be considered roughly as having an $N\pi$ component and a spin-$\frac{3}{2}$ three-quark component, only coupling to this last component is certainly free of "double-counting." This means that the coupling constants that strictly must be used are "partial" couplings, like for instance quark-model couplings. They are usually less than the full couplings and so also here lies a possibility for softening the potentials from the isobars. These matters will be studied when we actually try to apply the potentials in a model fit to the NN data.

The diagrams we calculate are (i) the parallel and crossed $\pi\rho$ diagrams of the similar type of graphs that were calculated by Brueckner and Watson (BW) [7] for 2π potentials with nucleons in the intermediate states; and (ii) the iterated $\pi\rho$ diagrams of the type of graphs that were calculated by Taketani, Machida, and Ohnuma (TMO) [8] for 2π potentials with nucleons in the intermediate states. As this distinction is convenient as a means to denote the different contributions, we will adopt this nomenclature also in this paper. So we refer to the dif-

*Electronic mail: U634999@HNYKUN11.BITNET.

ferent potential contributions as a BW type and a TMO type according to the type of graph they correspond to.

The $\pi\rho$ potentials are calculated using the adiabatic approximation for the nucleons and isobars in the intermediate states. Thus, we neglect recoil energies in the intermediate states, but we give a proper treatment of the $a \equiv M_\Delta - M_N$ mass difference in the intermediate states. Included are the contributions of all planar (parallel BW and TMO diagrams) and crossed three-dimensional momentum-space $\pi\rho$ diagrams. The latter are rather important for having the complete isospin structure of the potentials. We also give the contributions of the $\pi\rho$ iterations, which can be subtracted or not, depending on whether one performs a coupled-channel calculation for, e.g., the $NN, N\Delta$ system, or a single NN-channel calculation.

The paper is organized as follows. In Sec. II the $\pi\rho$-exchange kernels are derived for the NN sector. We give the interaction Lagrangians and we briefly indicate the implementation of the Gaussian form factors. In Sec. III the definition of the nucleon-nucleon $\pi\rho$ potential for the Lippmann-Schwinger equation is briefly repeated from [2] and the vertices in Pauli-spinor space are given for the $NN\pi$ and $N\Delta\pi$ as well as for the $NN\rho$ and $N\Delta\rho$ couplings. Here we also mention the approximations made in these vertices. Furthermore, we give the very useful spin projection operators for a spin-$\frac{1}{2}$ (nucleon) and a spin-$\frac{3}{2}$ (Δ-isobar) baryon, and the isospin factors.

In Sec. IV, using Appendix B, the $\pi\rho$ potentials are derived for the BW and TMO graphs for the $N\Delta$ and $\Delta\Delta$ intermediate states. We also present the iterated $\pi\rho$ kernels, i.e., the second-order Born terms. The $\pi\rho$ potentials with two nucleons in the intermediate state will be derived elsewhere [9]. In Sec. V the results are shown and discussed. In Appendix A, we review the Rarita-Schwinger formalism in some detail. This is useful for tracing the approximations we made at the vertices, in particular, in the case of the ρ couplings. In Appendix B, we give a dictionary of differentiation formulas, adequate for deriving the final form of the potentials of this paper in configuration space.

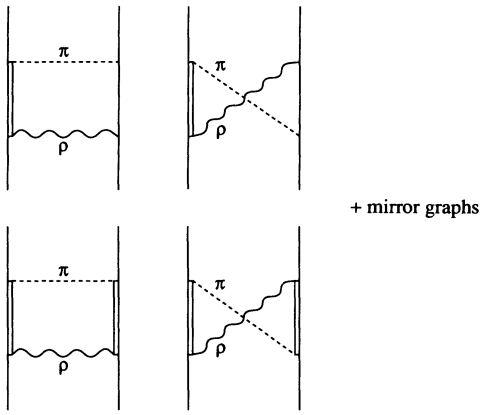

FIG. 1. Feynman diagrams for $\pi\rho$ exchange involving (a) one or (b) two Δ_{33}-isobar intermediate states.

II. THE $\pi\rho$-EXCHANGE NUCLEON-NUCLEON KERNEL

The two-meson-exchange kernel is written as a power series in λ, which denotes the number of baryon-baryon-meson (BBM) vertices. (For details and definitions we refer to Secs. III and IV of the companion paper [2].) The $\pi\rho$ contribution to the fourth-order λ terms of the two-meson-exchange kernel defines the $\pi\rho$-exchange potential. This corresponds to the planar- and crossed-box Feynman diagrams of Fig. 1. The corresponding fourth-order elastic NN-matrix element of the kernel is, as discussed in [2], given by

$$K^{(4)}(\mathbf{p}',\mathbf{p}|W)_{a'b';ab} = -(2\pi)^{-2}\,[W-\mathcal{W}(\mathbf{p}')]\,[W-\mathcal{W}(\mathbf{p})]\sum_{a'',b''}\int dp_0'\int dp_0\int dk_0\int dk_0'\int d\mathbf{k}\int d\mathbf{k}'$$

$$\times i(2\pi)^{-4}\delta^4(p-p'-k-k')[k'^2-m'^2+i\delta]^{-1}\left[F_W^{(a')}(\mathbf{p}',p_0')F_W^{(b')}(-\mathbf{p}',-p_0')\right]^{-1}$$

$$\times\Big\{[\Gamma_j\ F_W^{-1}(\mathbf{p}-\mathbf{k},p_0-k_0)\ \Gamma_i]^{(a'')}[\Gamma_j\ F_W^{-1}(-\mathbf{p}+\mathbf{k},-p_0+k_0)\ \Gamma_i]^{(b'')}$$

$$+[\Gamma_j\ F_W^{-1}(\mathbf{p}-\mathbf{k},p_0-k_0)\Gamma_i]^{(a'')}[\Gamma_i\ F_W^{-1}(-\mathbf{p}'-\mathbf{k},-p_0'-k_0)\Gamma_j]^{(b'')}\Big\}$$

$$\times\left[F_W^{(a)}(\mathbf{p},p_0)F_W^{(b)}(-\mathbf{p},-p_0)\right]^{-1}[k^2-m^2+i\delta]^{-1}\,. \qquad (2.1)$$

Here $a'', b'' = N, \Delta$ denote the baryons of the intermediate state. The Γ_i and Γ_j denote the baryon-baryon-meson vertices, which follow from the interaction Lagrangians (see below). The meson masses m and m' denote m_π or m_ρ. The c.m. momenta for the planar and crossed diagrams are indicated in Fig. 2. Note that the first term between the curly brackets corresponds to the planar-box $\pi\rho$-exchange diagram and the second term to the crossed-box $\pi\rho$-exchange diagram. In these diagrams only the contribution of the positive-energy nucleon and isobar states are included, in accordance with the pair-suppression hypothesis that we use in our work on two-meson exchange [1, 2].

The procedure to derive the kernels for the planar and crossed BW diagrams and for the TMO diagrams is amply described in Refs. [1, 2] and will not be repeated here.

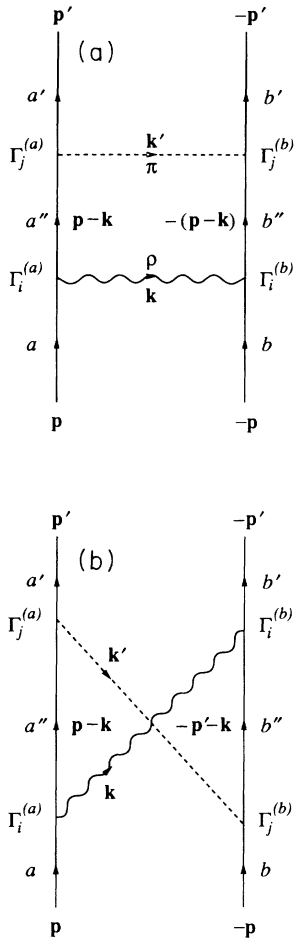

FIG. 2. Definition of momentum vectors in second-order (a) planar and (b) crossed graphs.

As discussed in these references, it suffices to evaluate one kernel for each particular set of diagrams. The other (mirror) diagrams in each set merely give rise to a factor of four when we evaluate the potentials. Furthermore, we get an additional factor of two from interchanging the π and ρ lines.

The vertices for the $\pi\rho$-exchange potentials are the $NN\pi$, ρ and $N\Delta\pi$, ρ vertices. For point couplings the Lagrangians are [10]

$$\mathcal{L}_{NN\pi} = \frac{f_{NN\pi}}{m_\pi}\overline{\psi}\gamma_5\gamma_\mu\boldsymbol{\tau}\psi\cdot\partial^\mu\boldsymbol{\phi}\ ,$$

$$\mathcal{L}_{N\Delta\pi} = \frac{f_{N\Delta\pi}}{m_\pi}\overline{\psi}\mathbf{T}\psi_\mu\cdot\partial^\mu\phi + \text{H.c.}\ ,$$

$$\mathcal{L}_{NN\rho} = \left[g_{NN\rho}\overline{\psi}\gamma_\mu\boldsymbol{\tau}\psi\cdot\boldsymbol{\rho}^\mu - \frac{f_{NN\rho}}{4M_N}\overline{\psi}\sigma_{\mu\nu}\boldsymbol{\tau}\psi\cdot(\partial^\nu\boldsymbol{\rho}^\mu - \partial^\mu\boldsymbol{\rho}^\nu)\right]\ ,$$

$$\mathcal{L}_{N\Delta\rho} = i\frac{f_{N\Delta\rho}}{m_\rho}\overline{\psi}\gamma_5\gamma_\nu\mathbf{T}\psi_\mu\cdot(\partial^\mu\boldsymbol{\rho}^\nu - \partial^\nu\boldsymbol{\rho}^\mu) + \text{H.c.}\ ,$$

where $\mathbf{T}$ is the isospin-$\frac{3}{2}$ isospin-$\frac{1}{2}$ transition operator and $\boldsymbol{\rho}^\mu$ is the ρ field. In momentum space this gives for the $NN\pi$ vertex

$$\bar{u}(\mathbf{p}')\Gamma u(\mathbf{p}) = i\left(\frac{f_{NN\pi}}{m_\pi}\right)\bar{u}(\mathbf{p}')\gamma_5\gamma\cdot(p-p')u(\mathbf{p})\ ,$$

for the $N\Delta\pi$ vertex

$$\bar{u}(\mathbf{p}')\Gamma^\mu u_\mu(\mathbf{p}) = i\left(\frac{f_{N\Delta\pi}}{m_\pi}\right)\bar{u}(\mathbf{p}')u_\mu(\mathbf{p})\cdot(p-p')^\mu\ ,$$

for the $NN\rho$ vertex

$$\bar{u}(\mathbf{p}')\Gamma u(\mathbf{p}) = \bar{u}(\mathbf{p}')\Big[\ g_{NN\rho}\gamma_\mu - \frac{if_{NN\rho}}{2M_N}\sigma_{\mu\nu}(p-p')^\nu\Big]\ u(\mathbf{p})\rho^\mu\ ,$$

and for the $N\Delta\rho$ vertex:

$$\bar{u}(\mathbf{p}')\Gamma^\mu u_\mu(\mathbf{p}) = \left(\frac{f_{N\Delta\rho}}{m_\rho}\right)\bar{u}(\mathbf{p}')\Big[\ \gamma_5\gamma_\nu(p-p')^\nu\rho^\mu - \gamma_5\gamma_\nu(p-p')^\mu\rho^\nu\Big]u_\mu(\mathbf{p}).$$

The generalization of the interaction kernels given above to the case with Gaussian form factors has been treated and explained in Refs. [1, 2]. The same procedure can be applied to the ρ exchange as well as to the π exchange. The form factors $F_\rho(\mathbf{k}^2)$ and $F_\pi(\mathbf{k}^2)$, which describe the ρ-exchange and π-exchange amplitudes, respectively, are simply a product of the Gaussian vertex form factors, e.g., $F_{NN\pi}(\mathbf{k}^2) = \exp(\mathbf{k}^2/2\Lambda^2_{NN\pi})$. In the NN sector we have for graphs with $N\Delta$ intermediate states,

$$\begin{aligned} F_\pi(\mathbf{k}^2) &= F_{N\Delta\pi}(\mathbf{k}^2)\ F_{NN\pi}(\mathbf{k}^2)\ , \\ F_\rho(\mathbf{k}^2) &= F_{N\Delta\rho}(\mathbf{k}^2)\ F_{NN\rho}(\mathbf{k}^2)\ , \end{aligned} \tag{2.2}$$

whereas for graphs with $\Delta\Delta$-intermediate states

$$F_\pi(\mathbf{k}^2) = F_{N\Delta\pi}(\mathbf{k}^2)^2,\quad F_\rho(\mathbf{k}^2) = F_{N\Delta\rho}(\mathbf{k}^2)^2\ . \tag{2.3}$$

III. THE NUCLEON-NUCLEON $\pi\rho$ POTENTIAL

The fourth-order potential $V^{(4)}$ consists of two parts. The first part is given by the fourth-order BW diagrams shown in Figs. 3 and 4. The second part comes from the TMO diagrams of Fig. 5, from which we have to subtract the iterated one-π and one-ρ contribution, so

$$V_{\rm TMO} = K_{\rm TMO} - K^{(2)}g\ K^{(2)}\ . \tag{3.1}$$

This will be henceforth referred to as the TMO contribution in analogy with the definition in Ref. [1]. Here, we restrict ourselves to the nucleon-nucleon sector. This implies that we do not consider the complete coupled-channel problem. Furthermore, in this paper we focus on the contributions to the NN potential due to the Δ_{33} isobar only up to fourth order. The only contributions

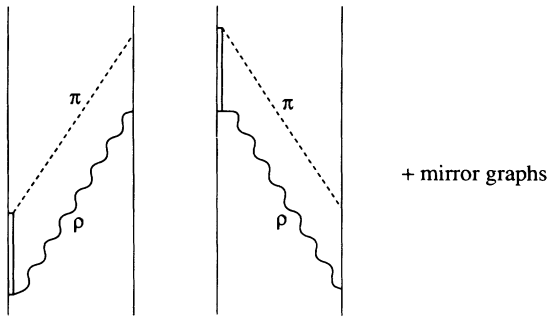

FIG. 3. Planar BW $\pi\rho$-exchange potential graphs with one Δ_{33} isobar in the intermediate state.

considered are the planar- and crossed-box diagrams with at least one Δ isobar in the intermediate state. (The diagrams with two nucleons in the intermediate state will be evaluated elsewhere [9].) Because it is supposed that the Lippmann-Schwinger equation is solved only in the nucleon-nucleon sector, the subtraction of the iterated one-meson exchange does not apply and $V^{(4)} = K^{(4)}$. For that purpose, in Sec. IV C we give the once-iterated π- and ρ-exchange kernels. These should be added to the TMO potential of Eq. (3.1) in order to compensate for the subtraction.

The transition from Dirac spinors to Pauli spinors is reviewed in Appendix C of [1]. There we derived the

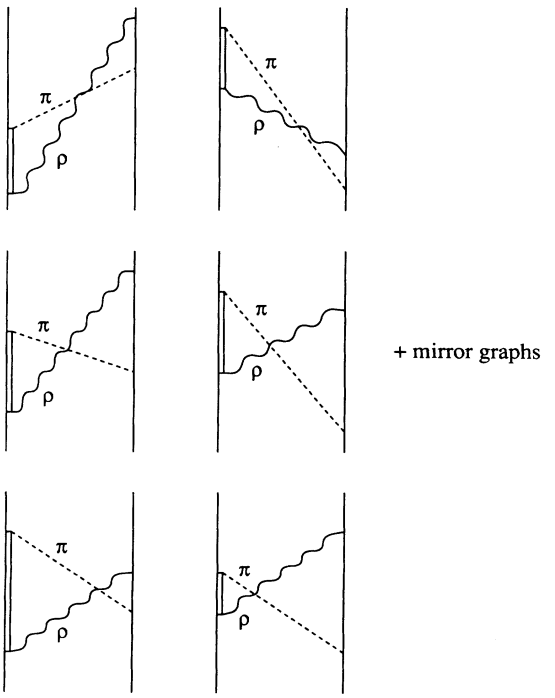

FIG. 4. Crossed BW $\pi\rho$-exchange potential graphs with one Δ_{33} isobar in the intermediate state.

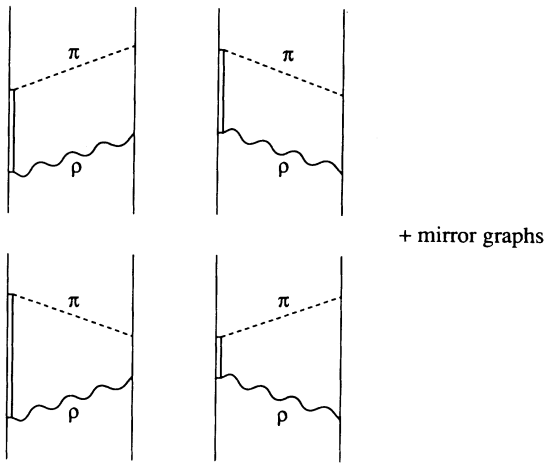

FIG. 5. TMO $\pi\rho$-exchange potential graphs with one Δ_{33} isobar in the intermediate state.

Lippmann-Schwinger equation

$$\chi(\mathbf{p}') = \chi^{(0)}(\mathbf{p}') + \tilde{g}(\mathbf{p}') \int d^3p \; \mathcal{V}(\mathbf{p}', \mathbf{p}) \chi(\mathbf{p}) \; , \quad (3.2)$$

for the Pauli-spinor wave functions $\chi(\mathbf{p})$. The wave function $\chi(\mathbf{p})$ and the potential $\mathcal{V}(\mathbf{p}', \mathbf{p})$ in the Pauli-spinor space are defined by

$$\phi(\mathbf{p}) = \sum_{\sigma_a, \sigma_b} \chi_{\sigma_a \sigma_b}(\mathbf{p}) \; u_a(\mathbf{p}, \sigma_a) u_b(-\mathbf{p}, \sigma_b) \; , \quad (3.3)$$

$$\chi^{(a)\dagger}_{\sigma'_a} \chi^{(b)\dagger}_{\sigma'_b} \; \mathcal{V} \; \chi^{(a)}_{\sigma_a} \chi^{(b)}_{\sigma_b} = \bar{u}_a(\mathbf{p}', \sigma'_a) \bar{u}_b(-\mathbf{p}', \sigma'_b) V(\mathbf{p}', \mathbf{p}) \times u_a(\mathbf{p}, \sigma_a) u_b(-\mathbf{p}, \sigma_b) \; . \quad (3.4)$$

Like in the derivation of the one-boson-exchange potentials [11, 12], we make the approximation

$$E(\mathbf{p}) = (\mathbf{p}^2 + M^2)^{1/2} \approx M + \mathbf{p}^2/2M$$

everywhere in the interaction kernels of Sec. IV, which of course is fully justified for low energies only. We have a similar expansion of the on-shell energy

$$W = 2(\mathbf{p}_i^2 + M^2)^{1/2} \approx 2M + \mathbf{p}_i^2/M \; .$$

In contrast to these kinds of approximations, the full $\mathbf{k}^2$ dependence of the form factors is kept throughout the derivation of the two-meson-exchange potential. Note that the Gaussian form factors strongly suppress the high-momentum transfers. This means that the contribution to the potentials from intermediate states which are far off energy shell cannot be very large.

The reduction of the two-meson-exchange potential from Dirac-spinor space to Pauli-spinor space is completely similar to the procedures discussed in Refs. [1, 2]. The vertex operators in Pauli-spinor space up to order $1/M$ are given by

(i) $NN\pi$ vertices:

$$\bar{u}(\mathbf{p}')\Gamma^{(a)}(\mathbf{p}',\mathbf{p})u(\mathbf{p}) = +i\left(\frac{f_{NN\pi}}{m_\pi}\right)\left[\boldsymbol{\sigma}_1\cdot\mathbf{k}\mp\frac{\omega}{2M_N}\boldsymbol{\sigma}_1\cdot(\mathbf{p}'+\mathbf{p})\right],$$
$$\bar{u}(-\mathbf{p}')\Gamma^{(b)}(\mathbf{p}',\mathbf{p})u(-\mathbf{p}) = -i\left(\frac{f_{NN\pi}}{m_\pi}\right)\left[\boldsymbol{\sigma}_2\cdot\mathbf{k}\mp\frac{\omega}{2M_N}\boldsymbol{\sigma}_2\cdot(\mathbf{p}'+\mathbf{p})\right], \tag{3.5}$$

(ii) $N\Delta\pi$ vertices:

$$\bar{u}(\mathbf{p}')\Gamma^{(a)}_\mu(\mathbf{p}',\mathbf{p})u^\mu(\mathbf{p}) = -i\left(\frac{f_{N\Delta\pi}}{m_\pi}\right)\boldsymbol{\Sigma}_1^\dagger\cdot\mathbf{k},$$
$$\bar{u}(-\mathbf{p}')\Gamma^{(b)}_\mu(\mathbf{p}',\mathbf{p})u^\mu(-\mathbf{p}) = +i\left(\frac{f_{N\Delta\pi}}{m_\pi}\right)\boldsymbol{\Sigma}_2^\dagger\cdot\mathbf{k}, \tag{3.6}$$

(iii) $NN\rho$ vertices:

$$\bar{u}(\mathbf{p}')\Gamma^{(a)}(\mathbf{p}',\mathbf{p})u(\mathbf{p}) = g_{NN\rho}\rho^0 - \left[\frac{g_{NN\rho}}{2M_N}(\mathbf{p}+\mathbf{p}')+i\frac{(g+f)_{NN\rho}}{2M_N}\mathbf{k}\times\boldsymbol{\sigma}_1\right]\cdot\boldsymbol{\rho},$$
$$\bar{u}(-\mathbf{p}')\Gamma^{(b)}(\mathbf{p}',\mathbf{p})u(-\mathbf{p}) = g_{NN\rho}\rho^0 + \left[\frac{g_{NN\rho}}{2M_N}(\mathbf{p}+\mathbf{p}')+i\frac{(g+f)_{NN\rho}}{2M_N}\mathbf{k}\times\boldsymbol{\sigma}_2\right]\cdot\boldsymbol{\rho}, \tag{3.7}$$

(iv) $N\Delta\rho$ vertices:

$$\bar{u}(\mathbf{p}')\Gamma^{(a)}_\mu(\mathbf{p}',\mathbf{p})u^\mu(\mathbf{p}) = +\left(\frac{f_{N\Delta\rho}}{m_\rho}\right)\left[-\boldsymbol{\sigma}_1\cdot\mathbf{k}\boldsymbol{\Sigma}_1^\dagger\cdot\boldsymbol{\rho}+\boldsymbol{\sigma}_1\cdot\boldsymbol{\rho}\boldsymbol{\Sigma}_1^\dagger\cdot\mathbf{k}-\frac{1}{4M_{N\Delta}}\boldsymbol{\sigma}_1\cdot(\mathbf{p}+\mathbf{p}')\boldsymbol{\Sigma}_1^\dagger\cdot\mathbf{k}\rho^0\right],$$
$$\bar{u}(-\mathbf{p}')\Gamma^{(b)}_\mu(\mathbf{p}',\mathbf{p})u^\mu(-\mathbf{p}) = -\left(\frac{f_{N\Delta\rho}}{m_\rho}\right)\left[-\boldsymbol{\sigma}_2\cdot\mathbf{k}\boldsymbol{\Sigma}_2^\dagger\cdot\boldsymbol{\rho}+\boldsymbol{\sigma}_2\cdot\boldsymbol{\rho}\boldsymbol{\Sigma}_2^\dagger\cdot\mathbf{k}+\frac{1}{4M_{N\Delta}}\boldsymbol{\sigma}_2\cdot(\mathbf{p}+\mathbf{p}')\boldsymbol{\Sigma}_2^\dagger\cdot\mathbf{k}\rho^0\right], \tag{3.8}$$

$\mathbf{k}\equiv\mathbf{p}-\mathbf{p}'$ and $M_{N\Delta}=M_NM_\Delta/(M_N+M_\Delta)$. For the Γ-matrix elements in Eq. (3.6), the upper sign applies for the creation and the lower sign for the absorption of the pion at the vertex. Note that for line (a) and line (b) we have used respectively the subscript 1 and 2 for the $\boldsymbol{\sigma}$ and $\boldsymbol{\Sigma}$ operators. For the Δ vertices we used the Rarita-Schwinger representation of the Δ isobar, which is reviewed in Appendix A. In the following we will neglect the contributions from the ρ^0 pieces in the diagrams with two Δ isobars in the intermediate states, since they are small due to the $1/M_{N\Delta}$ factors.

Useful for the evaluation of the second-order diagrams are the relations

$$\sigma_j\sigma_i=\delta_{ij}+i\epsilon_{jik}\sigma_k\,,\qquad \Sigma_j|\sigma\rangle\langle\sigma|\Sigma_i^\dagger=\tfrac{2}{3}\delta_{ij}-\tfrac{i}{3}\epsilon_{jik}\sigma_k\,. \tag{3.9}$$

Products of this type will occur for each baryon line. Identical formulas hold for the isospin operators $\boldsymbol{\tau}_i$ and $\mathbf{T}_i$. Using Eq. (3.9) for the latter, the isospin factors for the planar and the crossed diagrams can readily be evaluated. One finds for one Δ isobar in the intermediate state for the planar $(//)$ and the crossed (X) graph

$$C^{(//)}_{N\Delta}(I)=2+\tfrac{2}{3}\boldsymbol{\tau}_1\cdot\boldsymbol{\tau}_2,\quad C^{(X)}_{N\Delta}(I)=2-\tfrac{2}{3}\boldsymbol{\tau}_1\cdot\boldsymbol{\tau}_2\,, \tag{3.10}$$

where I denotes the total isospin of the NN state. For two Δ isobars in the intermediate state one gets for the planar and the crossed graphs

$$C^{(//)}_{\Delta\Delta}(I)=\tfrac{4}{3}-\tfrac{2}{9}\boldsymbol{\tau}_1\cdot\boldsymbol{\tau}_2,\quad C^{(X)}_{\Delta\Delta}(I)=\tfrac{4}{3}+\tfrac{2}{9}\boldsymbol{\tau}_1\cdot\boldsymbol{\tau}_2\,. \tag{3.11}$$

In this paper, we will restrict ourselves to the adiabatic approximation. In order to obtain the contributions to the potentials in the adiabatic approximation, we expand the energy denominators in the expressions for the planar- and crossed-box diagram and keep only the leading term. For details see Ref. [2]. As an example, a typical energy denominator is

$$\frac{1}{E_{\mathbf{p}}+\mathcal{E}_{\mathbf{p}-\mathbf{k}}-W+\omega}\approx\frac{1}{\omega+a}\,, \tag{3.12}$$

where $a=M_\Delta-M_N$. In the evaluation of the TMO graphs, we encounter the intermediate-state energy denominator $[\mathcal{E}_{\mathbf{p}-\mathbf{k}}+E_{\mathbf{p}-\mathbf{k}}-W]^{-1}$, the treatment of which is explained in Appendix A of the companion paper [2].

IV. $\pi\rho$-EXCHANGE POTENTIALS

Analogous to the evaluation of the 2π-exchange potential in the companion paper [1], the $\pi\rho$-exchange potential

can be easily obtained. In the following the index 1 in $\mathbf{k}_1, \omega_1$ refers to the ρ meson, and the index 2 in $\mathbf{k}_2, \omega_2$ refers to the π meson. As already stated, the interchange of the meson lines merely gives rise to an overall factor of 2.

A. NΔ graphs

The evaluation of the planar BW graphs of Fig. 3, the crossed BW graphs of Fig. 4, and the TMO graphs of Fig. 5 result in

$$V_{N\Delta}(\mathrm{BW}_{//}) = C_{N\Delta}^{(//)}(I)\frac{f_{N\Delta\rho}}{m_\rho}\frac{f_{N\Delta\pi}}{m_\pi}\frac{f_{NN\pi}}{m_\pi}\int\int\frac{d^3k_1 d^3k_2}{(2\pi)^6}e^{i(\mathbf{k}_1+\mathbf{k}_2)\cdot\mathbf{r}}F_\rho(\mathbf{k}_1^2)F_\pi(\mathbf{k}_2^2)$$
$$\times\left[\left\{\frac{1}{3}(\mathbf{k}_1\cdot\mathbf{k}_2)\boldsymbol{\sigma}_1-\frac{1}{3}(\boldsymbol{\sigma}_1\cdot\mathbf{k}_1)\mathbf{k}_2+\frac{2i}{3}\mathbf{k}_1\times\mathbf{k}_2\right\}(\boldsymbol{\sigma}_2\cdot\mathbf{k}_2)\cdot\left\{\frac{g_{NN\rho}}{2M_N}\mathbf{k}_2-i\frac{(g+f)_{NN\rho}}{2M_N}(\boldsymbol{\sigma}_2\times\mathbf{k}_1)\right\}\right.$$
$$\left.+\frac{g_{NN\rho}}{4M_{N\Delta}}\left\{\frac{1}{3}(\mathbf{k}_1\cdot\mathbf{k}_2)(\boldsymbol{\sigma}_1\cdot\mathbf{k}_2)+\frac{1}{3}\mathbf{k}_2^2(\boldsymbol{\sigma}_1\cdot\mathbf{k}_1)\right\}(\boldsymbol{\sigma}_2\cdot\mathbf{k}_2)\right]D^{(1)}_{\mathrm{BW}_{//}}(\omega_1,\omega_2)\ , \tag{4.1}$$

$$V_{N\Delta}(\mathrm{BW}_X) = C_{N\Delta}^{(X)}(I)\frac{f_{N\Delta\rho}}{m_\rho}\frac{f_{N\Delta\pi}}{m_\pi}\frac{f_{NN\pi}}{m_\pi}\int\int\frac{d^3k_1 d^3k_2}{(2\pi)^6}e^{i(\mathbf{k}_1+\mathbf{k}_2)\cdot\mathbf{r}}F_\rho(\mathbf{k}_1^2)F_\pi(\mathbf{k}_2^2)$$
$$\times\left[-\left\{\frac{1}{3}(\mathbf{k}_1\cdot\mathbf{k}_2)\boldsymbol{\sigma}_1-\frac{1}{3}(\boldsymbol{\sigma}_1\cdot\mathbf{k}_1)\mathbf{k}_2+\frac{2i}{3}\mathbf{k}_1\times\mathbf{k}_2\right\}\cdot\left\{\frac{g_{NN\rho}}{2M_N}\mathbf{k}_2+i\frac{(g+f)_{NN\rho}}{2M_N}(\boldsymbol{\sigma}_2\times\mathbf{k}_1)\right\}(\boldsymbol{\sigma}_2\cdot\mathbf{k}_2)\right.$$
$$\left.+\frac{g_{NN\rho}}{4M_{N\Delta}}\left\{\frac{1}{3}(\mathbf{k}_1\cdot\mathbf{k}_2)(\boldsymbol{\sigma}_1\cdot\mathbf{k}_2)+\frac{1}{3}\mathbf{k}_2^2(\boldsymbol{\sigma}_1\cdot\mathbf{k}_1)\right\}(\boldsymbol{\sigma}_2\cdot\mathbf{k}_2)\right]D^{(1)}_{\mathrm{BW}_X}(\omega_1,\omega_2)\ , \tag{4.2}$$

$$V_{N\Delta}(\mathrm{TMO}) = C_{N\Delta}^{(//)}(I)\frac{f_{N\Delta\rho}}{m_\rho}\frac{f_{N\Delta\pi}}{m_\pi}\frac{f_{NN\pi}}{m_\pi}\int\int\frac{d^3k_1 d^3k_2}{(2\pi)^6}e^{i(\mathbf{k}_1+\mathbf{k}_2)\cdot\mathbf{r}}F_\rho(\mathbf{k}_1^2)F_\pi(\mathbf{k}_2^2)$$
$$\times\left[\left\{\frac{1}{3}(\mathbf{k}_1\cdot\mathbf{k}_2)\boldsymbol{\sigma}_1-\frac{1}{3}(\boldsymbol{\sigma}_1\cdot\mathbf{k}_1)\mathbf{k}_2+\frac{2i}{3}\mathbf{k}_1\times\mathbf{k}_2\right\}(\boldsymbol{\sigma}_2\cdot\mathbf{k}_2)\cdot\left\{\frac{g_{NN\rho}}{2M_N}\mathbf{k}_2-i\frac{(g+f)_{NN\rho}}{2M_N}(\boldsymbol{\sigma}_2\times\mathbf{k}_1)\right\}\right.$$
$$\left.+\frac{g_{NN\rho}}{4M_{N\Delta}}\left\{\frac{1}{3}(\mathbf{k}_1\cdot\mathbf{k}_2)(\boldsymbol{\sigma}_1\cdot\mathbf{k}_2)+\frac{1}{3}\mathbf{k}_2^2(\boldsymbol{\sigma}_1\cdot\mathbf{k}_1)\right\}(\boldsymbol{\sigma}_2\cdot\mathbf{k}_2)\right]D^{(1)}_{\mathrm{TMO}}(\omega_1,\omega_2)\ , \tag{4.3}$$

where the energy denominators $D_\alpha^{(1)}$ can be found in Table I. Note that there we have used some algebra to rewrite the expression for $D_X^{(1)}$ into a more transparent form. In the TMO graphs the intermediate-state energy denominator $\mathcal{E}_{\mathbf{p}-\mathbf{k}_1}+E_{\mathbf{p}-\mathbf{k}_1}-W$ is approximated by $(a-\beta_1)$ with $\beta_1=\mathbf{k}_1\cdot\mathbf{k}_2/\overline{M}$ and $\overline{M}=(M_\Delta+M_N)/2$. The form factors are defined according to $F_\rho(\mathbf{k}_1^2)=F_{NN\rho}(\mathbf{k}_1^2)F_{N\Delta\rho}(\mathbf{k}_1^2)$ and $F_\pi(\mathbf{k}_2^2)=F_{NN\pi}(\mathbf{k}_2^2)F_{N\Delta\pi}(\mathbf{k}_2^2)$.

In this paper we will not go into any of the details of the potentials. The procedures are entirely similar to those of the companion paper [2]. Therefore, we will give the information in such a form that the interested reader can easily derive the expressions for the potentials in configuration space from Eqs. (4.1), (4.2), and (4.3) using Tables I and II (introduced below) and Appendix B. Using a similar notation as in [2], we write

$$V_{N\Delta}(\alpha) = C_{N\Delta}^{(\alpha)}(I)\frac{f_{N\Delta\rho}}{m_\rho}\frac{f_{N\Delta\pi}}{m_\pi}\frac{f_{NN\pi}}{m_\pi}\frac{1}{6M_N}\int\int\frac{d^3k_1 d^3k_2}{(2\pi)^6}e^{i(\mathbf{k}_1+\mathbf{k}_2)\cdot\mathbf{r}}F_\rho(\mathbf{k}_1^2)F_\pi(\mathbf{k}_2^2)$$
$$\times\left[(g+f)_{NN\rho}O^{(\alpha)}_{N\Delta,m}(\mathbf{k}_1,\mathbf{k}_2)+g_{NN\rho}O^{(\alpha)}_{N\Delta,e}(\mathbf{k}_1,\mathbf{k}_2)\right]D_\alpha^{(1)}(\omega_1,\omega_2)\ , \tag{4.4}$$

where α denotes planar BW, crossed BW, or TMO. The expressions for $O^{(\alpha)}_{N\Delta,e}$ and $O^{(\alpha)}_{N\Delta,m}$ are given in Table II. They include the contributions from *all* graphs, i.e., the $\pi\rho$ as well as the $\rho\pi$ contributions, as well as the "mirror" graphs. They can easily be found by inspection of Eqs. (4.1), (4.2), and (4.3).

The separation of the $\mathbf{k}_1$ and $\mathbf{k}_2$ dependence can be achieved again as in Refs. [1] and [2]. In Table I, $D_X^{(1)}$ and $D^{(1)}_{\mathrm{TMO}}$ are already in a suitable form for the application of Appendix B of Ref. [2], while for $D_{//}^{(1)}$ one easily derives that

$$D^{(1)}_{\mathrm{BW}_{//}}=\frac{1}{\omega_1(\omega_1+a)\omega_2(\omega_2+a)}\left[\frac{2}{\omega_1+\omega_2}+\frac{a}{\omega_1\omega_2}\right]. \tag{4.5}$$

TABLE I. Adiabatic approximation of the energy denominators $D_\alpha^{(1)}$ for the $N\Delta$ and $D_\alpha^{(2)}$ for the $\Delta\Delta$ intermediate states. Here $\beta_1 = \mathbf{k}_1 \cdot \mathbf{k}_2/\overline{M}$ and $\beta_2 = \mathbf{k}_1 \cdot \mathbf{k}_2/M_\Delta$.

α	$D_\alpha^{(1)}(\omega_1,\omega_2)$
$BW_{//}$	$\frac{1}{\omega_1\omega_2}\left[\frac{1}{(\omega_1+a)\omega_2}+\frac{1}{\omega_1(\omega_2+a)}\right]\frac{1}{(\omega_1+\omega_2)}$
BW_X	$\frac{2}{\omega_1\omega_2}\left[\frac{-1}{(\omega_1+a)(\omega_2+a)}\frac{1}{(\omega_1+\omega_2)}+\frac{1}{\omega_1\omega_2}\left(\frac{1}{\omega_1+a}+\frac{1}{\omega_2+a}-\frac{a}{(\omega_1+a)(\omega_2+a)}\right)\right]$
TMO	$\frac{1}{2\omega_1\omega_2}\left[\frac{1}{(\omega_1+a)\omega_2}\left(\frac{1}{\omega_1+a}+\frac{1}{\omega_2}\right)+\frac{1}{\omega_1(\omega_2+a)}\left(\frac{1}{\omega_2+a}+\frac{1}{\omega_1}\right)+\frac{1}{\omega_1\omega_2}\left(\frac{1}{\omega_1}+\frac{1}{\omega_2}\right)+\frac{1}{(\omega_1+a)(\omega_2+a)}\left(\frac{1}{\omega_1+a}+\frac{1}{\omega_2+a}\right)\right]\frac{\beta_1}{a-\beta_1}$
Born	$\frac{1}{\omega_1\omega_2}\left[\frac{1}{(\omega_1+a)\omega_2}+\frac{1}{\omega_1(\omega_2+a)}+\frac{1}{(\omega_1+a)(\omega_2+a)}+\frac{1}{\omega_1\omega_2}\right]\frac{1}{a-\beta_1}$

α	$D_\alpha^{(2)}(\omega_1,\omega_2)$
$BW_{//}$	$\frac{1}{\omega_1\omega_2}\left[\frac{1}{(\omega_1+a)(\omega_2+a)}\right]\frac{1}{(\omega_1+\omega_2)}$
BW_X	$-\frac{1}{\omega_1\omega_2}\frac{d}{da}\left[\frac{a}{(\omega_1+a)(\omega_2+a)(\omega_1+\omega_2)}+\frac{1}{(\omega_1+a)(\omega_2+a)}\right]$
TMO	$\frac{1}{2\omega_1\omega_2}\left[\frac{1}{(\omega_1+a)^2(\omega_2+a)}+\frac{1}{(\omega_1+a)(\omega_2+a)^2}\right]\frac{\beta_2}{2a-\beta_2}$
Born	$\frac{2}{\omega_1\omega_2}\left[\frac{1}{(\omega_1+a)(\omega_2+a)}\right]\frac{1}{2a-\beta_2}$

TABLE II. Momentum operators $O^{(\alpha)}(\mathbf{k}_1,\mathbf{k}_2)$ of the planar ($BW_{//}$ and TMO) and crossed (BW_X) graphs for the $N\Delta$ and $\Delta\Delta$ intermediate states. The indices e and m refer to the (electric) $g_{NN\rho}$ and (magnetic) $(g+f)_{NN\rho}$ parts.

α	$O_{N\Delta}(\mathbf{k}_1,\mathbf{k}_2)$
$O_{N\Delta,e}^{(//)}$	$-\frac{1}{2}\left[1-\frac{M_N}{M_\Delta}\right](\sigma_1\cdot\mathbf{k}_1)(\sigma_2\cdot\mathbf{k}_2)\mathbf{k}_2^2+\frac{1}{2}\left[3+\frac{M_N}{M_\Delta}\right](\sigma_1\cdot\mathbf{k}_2)(\sigma_2\cdot\mathbf{k}_2)(\mathbf{k}_1\cdot\mathbf{k}_2)$
$O_{N\Delta,m}^{(//)}$	$i(\sigma_1\cdot\mathbf{k}_1)(\sigma_2\cdot\mathbf{k}_2)(\sigma_2\cdot\mathbf{k}_1\times\mathbf{k}_2)+i(\mathbf{k}_1\cdot\mathbf{k}_2)(\sigma_2\cdot\mathbf{k}_2)(\sigma_2\cdot\sigma_1\times\mathbf{k}_1)$ $+2(\sigma_2\cdot\mathbf{k}_2)(\sigma_2\times\mathbf{k}_1\cdot\mathbf{k}_1\times\mathbf{k}_2)$
$O_{N\Delta,e}^{(X)}$	$+\frac{1}{2}\left[3+\frac{M_N}{M_\Delta}\right](\sigma_1\cdot\mathbf{k}_1)(\sigma_2\cdot\mathbf{k}_2)\mathbf{k}_2^2-\frac{1}{2}\left[1-\frac{M_N}{M_\Delta}\right](\sigma_1\cdot\mathbf{k}_2)(\sigma_2\cdot\mathbf{k}_2)(\mathbf{k}_1\cdot\mathbf{k}_2)$
$O_{N\Delta,m}^{(X)}$	$i(\sigma_1\cdot\mathbf{k}_1)(\sigma_2\cdot\mathbf{k}_1\times\mathbf{k}_2)(\sigma_2\cdot\mathbf{k}_2)+i(\mathbf{k}_1\cdot\mathbf{k}_2)(\sigma_2\cdot\sigma_1\times\mathbf{k}_1)(\sigma_2\cdot\mathbf{k}_2)$ $+2(\sigma_2\times\mathbf{k}_1\cdot\mathbf{k}_1\times\mathbf{k}_2)(\sigma_2\cdot\mathbf{k}_2)$

α	$O_{\Delta\Delta}(\mathbf{k}_1,\mathbf{k}_2)$
$O_{\Delta\Delta}^{(//)}$	$(\mathbf{k}_1\cdot\mathbf{k}_2)^2(\sigma_1\cdot\sigma_2)-(\mathbf{k}_1\cdot\mathbf{k}_2)(\sigma_1\cdot\mathbf{k}_2)(\sigma_2\cdot\mathbf{k}_1)-(\mathbf{k}_1\cdot\mathbf{k}_2)(\sigma_1\cdot\mathbf{k}_1)(\sigma_2\cdot\mathbf{k}_2)$ $+\mathbf{k}_2^2(\sigma_1\cdot\mathbf{k}_1)(\sigma_2\cdot\mathbf{k}_1)-4(\mathbf{k}_1\times\mathbf{k}_2)^2$
$O_{\Delta\Delta}^{(X)}$	$(\mathbf{k}_1\cdot\mathbf{k}_2)^2(\sigma_1\cdot\sigma_2)-(\mathbf{k}_1\cdot\mathbf{k}_2)(\sigma_1\cdot\mathbf{k}_2)(\sigma_2\cdot\mathbf{k}_1)-(\mathbf{k}_1\cdot\mathbf{k}_2)(\sigma_1\cdot\mathbf{k}_1)(\sigma_2\cdot\mathbf{k}_2)$ $+\mathbf{k}_2^2(\sigma_1\cdot\mathbf{k}_1)(\sigma_2\cdot\mathbf{k}_1)+4(\mathbf{k}_1\times\mathbf{k}_2)^2$

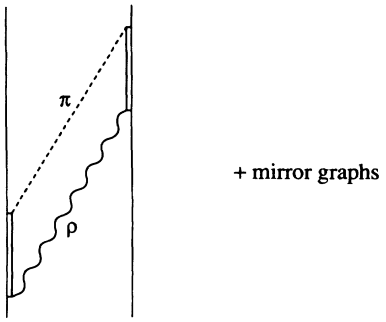

FIG. 6. Planar BW $\pi\rho$-exchange potential graphs with two Δ_{33} isobars in the intermediate state.

Now, all momentum integrals can be written in terms of the functions $G_{m,n}(a,r)$ and $H_{m,n}(a,r_1,r_2)$ of Appendix B of Ref. [2]. For that purpose, we write

$$e^{i(\mathbf{k}_1+\mathbf{k}_2)\cdot\mathbf{r}} = \lim_{\mathbf{r}_1,\mathbf{r}_2\to\mathbf{r}} e^{i\mathbf{k}_1\cdot\mathbf{r}_1} e^{i\mathbf{k}_2\cdot\mathbf{r}_2} , \tag{4.6}$$

and take the limit operation before the momentum integrations. Next, we replace all momenta occurring in the numerator by ∇_1 and ∇_2 operations, which are the ∇ operations with respect to $\mathbf{r}_1$ and $\mathbf{r}_2$, respectively, and take these in front of the momentum integrations. After the momentum integrations we perform the differentiations and take the limit. In view of these operations, we can write Eq. (4.4) in the form

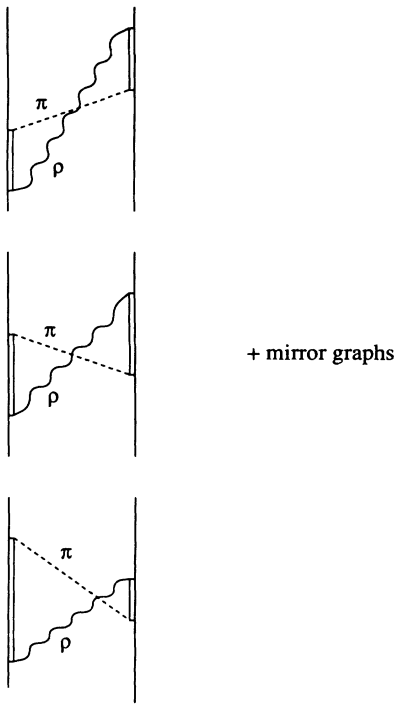

FIG. 7. Crossed BW $\pi\rho$-exchange potential graphs with two Δ_{33} isobars in the intermediate state.

$$V_{N\Delta}(\alpha) = C^{(\alpha)}_{N\Delta}(I)\frac{f_{N\Delta\rho}}{m_\rho}\frac{f_{N\Delta\pi}}{m_\pi}\frac{f_{NN\pi}}{m_\pi}\ \frac{1}{6M_N}\lim_{\mathbf{r}_1,\mathbf{r}_2\to\mathbf{r}}\left[(g+f)_{NN\rho}O^{(\alpha)}_{N\Delta,m}(\nabla_1,\nabla_2)+g_{NN\rho}O^{(\alpha)}_{N\Delta,e}(\nabla_1,\nabla_2)\right]B^{(\alpha)}_{N\Delta}(r_1,r_2) , \tag{4.7}$$

where

$$B^{(\mathrm{BW}//)}_{N\Delta}(r_1,r_2) = 2H_{1,1}(a;r_1,r_2)+aG_{2,1}(a,r_1)G_{2,1}(a,r_2) ,$$

$$B^{(\mathrm{BW}x)}_{N\Delta}(r_1,r_2) = -2H_{1,1}(a;r_1,r_2)+2G_{2,1}(a,r_1)I_2(m_\pi,r_2)+2I_2(m_\rho,r_1)G_{2,1}(a,r_2)-2aG_{2,1}(a,r_1)G_{2,1}(a,r_2) ,$$

$$\begin{aligned}B^{(\mathrm{TMO})}_{N\Delta}(r_1,r_2) = &-\tfrac{1}{2}[G_{1,2}(a,r_1)I_2(m_\pi,r_2)+G_{1,1}(a,r_1)I_3(m_\pi,r_2)+I_3(m_\rho,r_1)I_2(m_\pi,r_2)+G_{1,2}(a,r_1)G_{1,1}(a,r_2)]\\ &+a\int_0^\infty dz\, e^{-z(a-\frac{1}{2}T_{\mathrm{lab}})}\tfrac{1}{2}[G_{1,2}(z;a,r_1)I_2(z;m_\pi,r_2)\\ &\quad+G_{1,1}(z;a,r_1)I_3(z;m_\pi,r_2)+I_3(z;m_\rho,r_1)I_2(z;m_\pi,r_2)\\ &\quad+G_{1,2}(z;a,r_1)G_{1,1}(z;a,r_2)]+(m_\rho\leftrightarrow m_\pi) .\end{aligned} \tag{4.8}$$

In Appendix B of this paper we give a set of explicit formulas such that the result for $O^{(\alpha)}_{N\Delta}(\nabla_1,\nabla_2)F(r_1)G(r_2)$ can be written down immediately. Here and in the following, we refrain from giving the full detailed result, since this is not particularly illuminating. Moreover, the potentials can be evaluated rather easily by an interested reader.

B. $\Delta\Delta$ graphs

The evaluation of the planar BW graphs of Fig. 6, the crossed BW graphs of Fig. 7, and the TMO graphs of Fig. 8 result in

$$V_{\Delta\Delta}(\mathrm{BW}_{//}) = C^{(//)}_{\Delta\Delta}(I)\left(\frac{f_{N\Delta\rho}}{m_\rho}\right)^2\left(\frac{f_{N\Delta\pi}}{m_\pi}\right)^2\int\!\!\int \frac{d^3k_1 d^3k_2}{(2\pi)^6} e^{i(\mathbf{k}_1+\mathbf{k}_2)\cdot\mathbf{r}} F_\rho(\mathbf{k}_1^2)F_\pi(\mathbf{k}_2^2)$$
$$\times\left\{\frac{1}{3}(\mathbf{k}_1\cdot\mathbf{k}_2)\boldsymbol{\sigma}_1 - \frac{1}{3}(\boldsymbol{\sigma}_1\cdot\mathbf{k}_1)\mathbf{k}_2 + \frac{2i}{3}\mathbf{k}_1\times\mathbf{k}_2\right\}$$
$$\cdot\left\{\frac{1}{3}(\mathbf{k}_1\cdot\mathbf{k}_2)\boldsymbol{\sigma}_2 - \frac{1}{3}(\boldsymbol{\sigma}_2\cdot\mathbf{k}_1)\mathbf{k}_2 + \frac{2i}{3}\mathbf{k}_1\times\mathbf{k}_2\right\} D^{(2)}_{\mathrm{BW}_{//}}(\omega_1,\omega_2)\ , \tag{4.9}$$

$$V_{\Delta\Delta}(\mathrm{BW}_X) = C^{(X)}_{\Delta\Delta}(I)\left(\frac{f_{N\Delta\rho}}{m_\rho}\right)^2\left(\frac{f_{N\Delta\pi}}{m_\pi}\right)^2\int\!\!\int \frac{d^3k_1 d^3k_2}{(2\pi)^6} e^{i(\mathbf{k}_1+\mathbf{k}_2)\cdot\mathbf{r}} F_\rho(\mathbf{k}_1^2)F_\pi(\mathbf{k}_2^2)$$
$$\times\left\{\frac{1}{3}(\mathbf{k}_1\cdot\mathbf{k}_2)\boldsymbol{\sigma}_1 - \frac{1}{3}(\boldsymbol{\sigma}_1\cdot\mathbf{k}_1)\mathbf{k}_2 + \frac{2i}{3}\mathbf{k}_1\times\mathbf{k}_2\right\}$$
$$\cdot\left\{\frac{1}{3}(\mathbf{k}_1\cdot\mathbf{k}_2)\boldsymbol{\sigma}_2 - \frac{1}{3}(\boldsymbol{\sigma}_2\cdot\mathbf{k}_1)\mathbf{k}_2 - \frac{2i}{3}\mathbf{k}_1\times\mathbf{k}_2\right\} D^{(2)}_{\mathrm{BW}_X}(\omega_1,\omega_2)\ , \tag{4.10}$$

$$V_{\Delta\Delta}(\mathrm{TMO}) = C^{(//)}_{\Delta\Delta}(I)\left(\frac{f_{N\Delta\rho}}{m_\rho}\right)^2\left(\frac{f_{N\Delta\pi}}{m_\pi}\right)^2\int\!\!\int \frac{d^3k_1 d^3k_2}{(2\pi)^6} e^{i(\mathbf{k}_1+\mathbf{k}_2)\cdot\mathbf{r}} F_\rho(\mathbf{k}_1^2)F_\pi(\mathbf{k}_2^2)$$
$$\times\left\{\frac{1}{3}(\mathbf{k}_1\cdot\mathbf{k}_2)\boldsymbol{\sigma}_1 - \frac{1}{3}(\boldsymbol{\sigma}_1\cdot\mathbf{k}_1)\mathbf{k}_2 + \frac{2i}{3}\mathbf{k}_1\times\mathbf{k}_2\right\}$$
$$\cdot\left\{\frac{1}{3}(\mathbf{k}_1\cdot\mathbf{k}_2)\boldsymbol{\sigma}_2 - \frac{1}{3}(\boldsymbol{\sigma}_2\cdot\mathbf{k}_1)\mathbf{k}_2 + \frac{2i}{3}\mathbf{k}_1\times\mathbf{k}_2\right\} D^{(2)}_{\mathrm{TMO}}(\omega_1,\omega_2)\ , \tag{4.11}$$

where the energy denominators $D^{(2)}_\alpha$ can be found in Table I, and the form factors are $F_\rho(\mathbf{k}_1^2) = F_{N\Delta\rho}(\mathbf{k}_1^2)^2$ and $F_\pi(\mathbf{k}_2^2) = F_{N\Delta\pi}(\mathbf{k}_2^2)^2$. Following the same procedure as in the foregoing section, we write the potentials of Eqs. (4.9), (4.10), and (4.11) in the general form

$$V_{\Delta\Delta}(\alpha) = C^{(\alpha)}_{\Delta\Delta}(I)\left(\frac{f_{N\Delta\rho}}{m_\rho}\right)^2\left(\frac{f_{N\Delta\pi}}{m_\pi}\right)^2\frac{1}{9}\int\!\!\int \frac{d^3k_1 d^3k_2}{(2\pi)^6} e^{i(\mathbf{k}_1+\mathbf{k}_2)\cdot\mathbf{r}} F_\rho(\mathbf{k}_1^2)F_\pi(\mathbf{k}_2^2) O^{(\alpha)}_{\Delta\Delta}(\mathbf{k}_1,\mathbf{k}_2) D^{(2)}_\alpha(\omega_1,\omega_2)\ , \tag{4.12}$$

where the expressions for $O^{(\alpha)}_{\Delta\Delta}$ are given in Table II, again including the contributions from *all* graphs. Note the fact that terms with $(\mathbf{k}_1\cdot\mathbf{k}_2)(\boldsymbol{\sigma}_1 \pm \boldsymbol{\sigma}_2)\cdot\mathbf{k}_1\times\mathbf{k}_2$ give no contribution upon integration, hence they are omitted from Table II. Also, in Table I we have used some algebra to rewrite the expression for $D^{(2)}_X$ into a more transparent form. The Fourier transformations can now be easily read-off from the Tables I and II. Again, all momentum integrals can be written in terms of the functions $G_{m,n}(a,r)$ and $H_{m,n}(a,r_1,r_2)$. Following the same steps as in the preceding section, we write Eq. (4.12) in the form

$$V_{\Delta\Delta}(\alpha) = C^{(\alpha)}_{\Delta\Delta}(I)\left(\frac{f_{N\Delta\rho}}{m_\rho}\right)^2\left(\frac{f_{N\Delta\pi}}{m_\pi}\right)^2\frac{1}{9}\lim_{\mathbf{r}_1,\mathbf{r}_2\to\mathbf{r}} O^{(\alpha)}_{\Delta\Delta}(\boldsymbol{\nabla}_1,\boldsymbol{\nabla}_2) B^{(\alpha)}_{\Delta\Delta}(r_1,r_2)\ , \tag{4.13}$$

where

$$\begin{aligned}
B^{(\mathrm{BW}_{//})}_{\Delta\Delta}(r_1,r_2) &= H_{1,1}(a;r_1,r_2)\ ,\\
B^{(\mathrm{BW}_X)}_{\Delta\Delta}(r_1,r_2) &= -\frac{d}{da}\left[aH_{1,1}(a;r_1,r_2) + G_{1,1}(a,r_1)G_{1,1}(a,r_2)\right]\ ,\\
B^{(\mathrm{TMO})}_{\Delta\Delta}(r_1,r_2) &= -\tfrac{1}{2}\left[G_{1,1}(a,r_1)G_{1,2}(a,r_2) + G_{1,2}(a,r_1)G_{1,1}(a,r_2)\right]\\
&\quad + a\int_0^\infty dz e^{-z(2a-\frac{1}{2}T_{\mathrm{lab}})}\left[G_{1,1}(z;a,r_1)G_{1,2}(z;a,r_2) + G_{1,2}(z;a,r_1)G_{1,1}(z;a,r_2)\right]\ .
\end{aligned} \tag{4.14}$$

C. Iterated $\pi\rho$-exchange kernels

As in our previous paper [2], our definition of the TMO potential (3.1) explicitly contains the subtraction of the once-iterated one-meson-exchange kernels. In the case of a single-channel Lippmann-Schwinger or Schrödinger calculation for the NN channel, one should include only the pure TMO diagrams (and the BW diagrams, of course). Therefore, in this section we give the second-order Born approximation to the interaction kernels. These can then be added to the TMO potentials of Eqs. (4.7) and (4.13).

(i) $N\Delta$ *graphs*. The $N\Delta$ graph of Fig. 9 for both $\pi\rho$ and $\rho\pi$ exchange gives the kernel

$$K^{(4)}_{N\Delta}(\text{Born}) = C^{(//)}_{N\Delta}(I)\frac{f_{N\Delta\rho}}{m_\rho}\frac{f_{N\Delta\pi}}{m_\pi}\frac{f_{NN\pi}}{m_\pi}\int\int\frac{d^3k_1 d^3k_2}{(2\pi)^6}e^{i(\mathbf{k}_1+\mathbf{k}_2)\cdot\mathbf{r}}F_\rho(\mathbf{k}_1^2)F_\pi(\mathbf{k}_2^2)$$
$$\times\left[\left\{\frac{1}{3}(\mathbf{k}_1\cdot\mathbf{k}_2)\boldsymbol{\sigma}_1-\frac{1}{3}(\boldsymbol{\sigma}_1\cdot\mathbf{k}_1)\mathbf{k}_2+\frac{2i}{3}\mathbf{k}_1\times\mathbf{k}_2\right\}(\boldsymbol{\sigma}_2\cdot\mathbf{k}_2)\cdot\left\{\frac{g_{NN\rho}}{2M_N}\mathbf{k}_2-i\frac{(g+f)_{NN\rho}}{2M_N}(\boldsymbol{\sigma}_2\times\mathbf{k}_1)\right\}\right.$$
$$\left.+\frac{g_{NN\rho}}{4M_{N\Delta}}\left\{\frac{1}{3}(\mathbf{k}_1\cdot\mathbf{k}_2)(\boldsymbol{\sigma}_1\cdot\mathbf{k}_2)+\frac{1}{3}\mathbf{k}_2^2(\boldsymbol{\sigma}_1\cdot\mathbf{k}_1)\right\}(\boldsymbol{\sigma}_2\cdot\mathbf{k}_2)\right]D^{(1)}_{\text{Born}}(\omega_1,\omega_2)\ , \tag{4.15}$$

where $F_\rho(\mathbf{k}_1^2)$ and $F_\pi(\mathbf{k}_2^2)$ are the same as in Sec. IV A. In the adiabatic approximation, which we will use henceforth, we have $\mathcal{E}_{\mathbf{p}-\mathbf{k}}+E_{\mathbf{p}-\mathbf{k}}-W\approx(a-\beta_1)$, the treatment of which can be found in Appendix A of Ref. [1]. We find

$$V^{(4)}_{N\Delta}(\text{Born}) = C^{(//)}_{N\Delta}(I)\frac{f_{N\Delta\rho}}{m_\rho}\frac{f_{N\Delta\pi}}{m_\pi}\frac{f_{NN\pi}}{m_\pi}\frac{1}{6M_N}\lim_{\mathbf{r}_1,\mathbf{r}_2\to\mathbf{r}}\left[g_{NN\rho}O^{(\alpha)}_{N\Delta,e}(\boldsymbol{\nabla}_1,\boldsymbol{\nabla}_2)(g+f)_{NN\rho}+O^{(\alpha)}_{N\Delta,m}(\boldsymbol{\nabla}_1,\boldsymbol{\nabla}_2)\right]$$
$$\times\int_0^\infty dz e^{-z(a-\frac{1}{2}T_{\text{lab}})}\left[G_{1,1}(z;a,r_1)I_2(z;m_\pi,r_2)+I_2(z;m_\rho,r_1)G_{1,1}(z;a,r_2)\right.$$
$$\left.+G_{1,1}(z;a,r_1)G_{1,1}(z;a,r_2)+I_2(z;m_\rho,r_1)I_2(z;m_\pi,r_2)\right]\ , \tag{4.16}$$

where the operators $O^{(\alpha)}_{N\Delta}$ are given in Table II.

(ii) $\Delta\Delta$ *graphs*. The $\Delta\Delta$ graph of Fig. 9 for both $\pi\rho$- and $\rho\pi$ exchange gives the kernel

$$K^{(4)}_{\Delta\Delta}(\text{Born}) = C^{(//)}_{\Delta\Delta}(I)\left(\frac{f_{N\Delta\rho}}{m_\rho}\right)^2\left(\frac{f_{N\Delta\pi}}{m_\pi}\right)^2\int\int\frac{d^3k_1 d^3k_2}{(2\pi)^6}e^{i(\mathbf{k}_1+\mathbf{k}_2)\cdot\mathbf{r}}F_\rho(\mathbf{k}_1^2)F_\pi(\mathbf{k}_2^2)$$
$$\times\left\{\frac{1}{3}(\mathbf{k}_1\cdot\mathbf{k}_2)\boldsymbol{\sigma}_1-\frac{1}{3}(\boldsymbol{\sigma}_1\cdot\mathbf{k}_1)\mathbf{k}_2+\frac{2i}{3}\mathbf{k}_1\times\mathbf{k}_2\right\}$$
$$\cdot\left\{\frac{1}{3}(\mathbf{k}_1\cdot\mathbf{k}_2)\boldsymbol{\sigma}_2-\frac{1}{3}(\boldsymbol{\sigma}_2\cdot\mathbf{k}_1)\mathbf{k}_2+\frac{2i}{3}\mathbf{k}_1\times\mathbf{k}_2\right\}D^{(2)}_{\text{Born}}(\omega_1,\omega_2)\ , \tag{4.17}$$

where $F_\rho(\mathbf{k}_1^2)$ and $F_\pi(\mathbf{k}_2^2)$ are the same as in Sec. IV B. The corresponding potential reads

$$V^{(4)}_{\Delta\Delta}(\text{Born}) = C^{(//)}_{\Delta\Delta}(I)\left(\frac{f_{N\Delta\rho}}{m_\rho}\right)^2\left(\frac{f_{N\Delta\pi}}{m_\pi}\right)^2\frac{1}{9}\lim_{\mathbf{r}_1,\mathbf{r}_2\to\mathbf{r}}O^{(\alpha)}_{\Delta\Delta}(\boldsymbol{\nabla}_1,\boldsymbol{\nabla}_2)$$
$$\times 2\int_0^\infty dz\, e^{-z(2a-\frac{1}{2}T_{\text{lab}})}G_{1,1}(z;a,r_1)G_{1,1}(z;a,r_2)\ , \tag{4.18}$$

where the operators $O^{(\alpha)}_{\Delta\Delta}$ are given in Table II.

So, for an $(NN,N\Delta)\to(NN,N\Delta)$ coupled-channel calculation the potential of Eq. (4.16) should be added to the TMO potential of Eq. (4.13) in order to compensate for the subtraction of the iterated $\pi\rho$ exchange with two Δ isobars in the intermediate states. For a single-channel NN calculation one has to add the potentials of both Eqs. (4.16) and (4.18) to the TMO potentials of Eqs. (4.7) and (4.13), respectively.

V. RESULTS AND DISCUSSION

The complete $\pi\rho$-exchange potential can be written as

$$V_i(\pi\rho) = V_i(\text{BW}) + V_i(\text{TMO}) + V_i(\text{Born})\ , \tag{5.1}$$

with $i = C, \sigma$, or T. Furthermore, each potential is the sum of the different contributions introduced in Sec. IV. The inclusion of the Born term $V_i(\text{Born})$ is due to our special definition of the TMO potential, Eq. (3.1), which

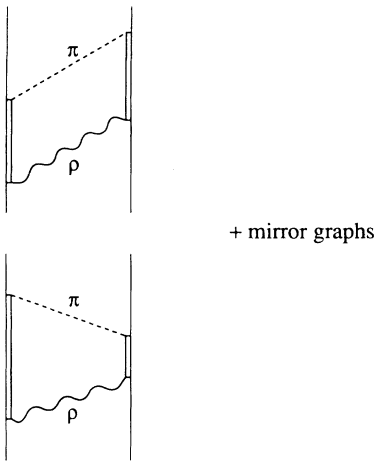

FIG. 8. TMO $\pi\rho$-exchange potential graphs with two Δ_{33} isobars in the intermediate state.

explicitly includes the subtraction of the once-iterated OPE. For a coupled-channel calculation this Born term should be left out. The iterated Born terms and $V_{\rm TMO}$ are energy dependent. We have evaluated the potentials for $T_{\rm lab} = 150$ MeV.

In Figs. 10–12 the results for the several potentials and several different combinations of contributions are shown. For π exchange we have used the same parameters as in [2], i.e., $f^2_{NN\pi}/4\pi = 0.075$, $f^2_{N\Delta\pi}/4\pi = 0.35$, and $\Lambda_\pi = 664.52$ MeV.

The $NN\rho$ coupling constants are taken from Ref. [11], so $g^2_{NN\rho}/4\pi = 0.795$, $(f/g)_{NN\rho} = 4.221$. The $N\Delta\rho$ coupling is taken from Ref. [13], where $f^2_{N\Delta\rho}/4\pi = 4.86$ was used. The form-factor mass for all the ρ vertices is taken to be $\Lambda_\rho = 464.52$ MeV. Like in the companion paper [2], we assumed that the strong form factor for the nucleon and the Δ_{33} isobar are the same. A motivation for $\Lambda_\rho < \Lambda_\pi$ is that the nucleon radius as seen by the ρ meson is larger than that for the π meson, since the ρ meson can couple to the pion cloud more easily than the π meson. A difference of about 200 MeV comes out in the Regge theory, where the π meson chooses the sense and the ρ meson the nonsense mechanism [14]. For larger Λ_ρ, the $\pi\rho$-exchange potentials become quite strong in the intermediate region. For example, for $\Lambda_\rho = \Lambda_\pi = 664.52$ MeV, we get $V_C(I=0) = 90$ MeV and $V_C(I=1) = 65$ MeV at $r = 1$ fm. However, preliminary calculations including the $\pi\rho$-exchange potential with NN intermediate states seem to indicate that large cancellations occur. The presentation of the $\pi\rho$- and all other π-meson-exchange potentials will be deferred to a future paper [9]. Here we only focus on the $\pi\rho$-exchange potential with at least one Δ isobar in the intermediate state.

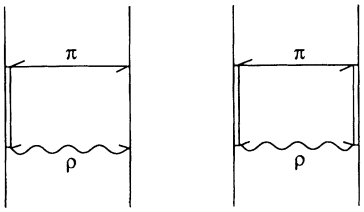

FIG. 9. Second-order potential scattering diagrams with (a) one or (b) two Δ_{33} isobars in the intermediate state.

Clearly the numerical results should be considered as illustrations. Certainly in the intermediate region one can trade off coupling constants and form factor masses. However, different coupling constants will give different potential tails. A better estimate of the $\pi\rho$-exchange potentials will be obtained after the confrontation of these new configuration-space potentials with the NN data.

In Figs. 10(a)–(d) we show the total isobar contributions, due to the $N\Delta$ and $\Delta\Delta$ intermediate states, for both the $\pi\rho$- and $\pi\pi$-exchange potentials. This for the central, spin-spin, and tensor potentials. Note the well-known strong cancellation between the $\pi\rho$ and $\pi\pi$ contributions for both $I = 0$ and $I = 1$ above $r = 0.75$ fm, which was already pointed out in the dispersion calculation of Ref. [3].

In Figs. 11(a) and (b) the BW, the TMO, and the Born contributions are compared. Like in the $\pi\pi$-exchange potential (see Ref. [2]), the $I = 0$ channel is strongly dominated by the BW graphs. In the $I = 1$ channel this is no longer the case. Here the iterated Born contribution is about equally important as the BW graphs.

In Figs. 12(a) and (b) we compare the electric $g_e = g_{NN\rho}$ and magnetic $g_m = (g+f)_{NN\rho}$ contributions as introduced in Eq. (4.7). The central potentials are strongly magnetically dominated. For the tensor potentials the electric and magnetic couplings are about equally important and of opposite sign, resulting in rather modest tensor $\pi\rho$-exchange potentials.

We have not displayed the differences between the $N\Delta$ and $\Delta\Delta$ contributions. These will be similar to those for the $\pi\pi$ potentials, which are shown in [2]. The same one also expects to hold for the energy dependence of the potentials.

This is the third paper in a series dealing with two-meson-exchange potentials in configuration space. Ultimately we plan to make a fit with the recent nucleon-nucleon phase-shift analyses of our group [15]. So apart from a pedagogical value, the results of this paper will play a role in our study of the nucleon-nucleon interaction, the coupling constants, and the role of resonances.

ACKNOWLEDGMENTS

We would like to thank Prof. J.J. de Swart and the other members of our group for their stimulating interest. We appreciated the help from Drs. C. Terheggen in making the figures. Part of this work was included in the research program of the Stichting voor Fundamenteel Onderzoek der Materie (FOM) with financial support from the Nederlandse Organisatie voor Wetenschappelijk Onderzoek (NWO).

APPENDIX A: RARITA-SCHWINGER SPINORS

The Rarita-Schwinger spinor for a spin-$\frac{3}{2}$ particle can be written as (see, e.g., Ref. [16])

$$u^\mu(p,\sigma) = L^{(3/2)}(p)^\mu_\nu \; u^\nu(0,\sigma) \; , \tag{A1}$$

where $u^\nu(0,\sigma)$ is the spinor in the Δ-isobar rest frame, and σ is its spin projection in that frame. Since one can construct the spin-$\frac{3}{2}$ states from the direct product of the spin-$\frac{1}{2}$ and spin-1 states [17], the boost operator in Eq. (A1) may be factorized according to

$$L^{(3/2)}(p)^\mu_\nu = L^{(1)}(p)^\mu_\nu \; L^{(1/2)}(p) \; , \tag{A2}$$

consisting of a boost for a spin-1 particle with mass M_Δ

$$L^{(1)}(p)^\mu_\nu = \begin{pmatrix} E/M_\Delta & p_j/M_\Delta \\ p^i/M_\Delta & \delta^i_j - p^i p_j [M_\Delta(E+M_\Delta)]^{-1} \end{pmatrix} \; , \tag{A3}$$

and a boost for spin-$\frac{1}{2}$ particle

$$L^{(1/2)}(p) \; u(0,\sigma) = \frac{(\gamma\cdot p + M_\Delta)}{[2M_\Delta(E+M_\Delta)]^{1/2}} u(0,\sigma)$$

$$= \left(\frac{E+M_\Delta}{2M_\Delta}\right)^{1/2} \begin{pmatrix} 1 \\ \dfrac{\boldsymbol{\sigma}\cdot\mathbf{p}}{E+M_\Delta} \end{pmatrix} \otimes \chi_\sigma \; . \tag{A4}$$

Here of course, χ_σ is the 2-component Pauli spinor. In the Δ-isobar rest frame, the $\frac{3}{2}$-spinor $u^\mu(0,\sigma)$ is also a 2-component spinor, which is related to the 4-component Pauli spinor ψ_σ of a spin-$\frac{3}{2}$ particle through the spin-$\frac{1}{2}$, spin-$\frac{3}{2}$ transition operators $\Sigma^\mu_{N\Delta}$ according to [16]

$$u^\mu(0,\sigma) = \left(\Sigma^\dagger_{N\Delta}\right)^\mu \psi_\sigma \; , \quad \Sigma^\dagger_{N\Delta} = (0, \boldsymbol{\Sigma}^\dagger) \; . \tag{A5}$$

So the Rarita-Schwinger spin-$\frac{3}{2}$ spinor in the Pauli-Dirac representation reads explicitly

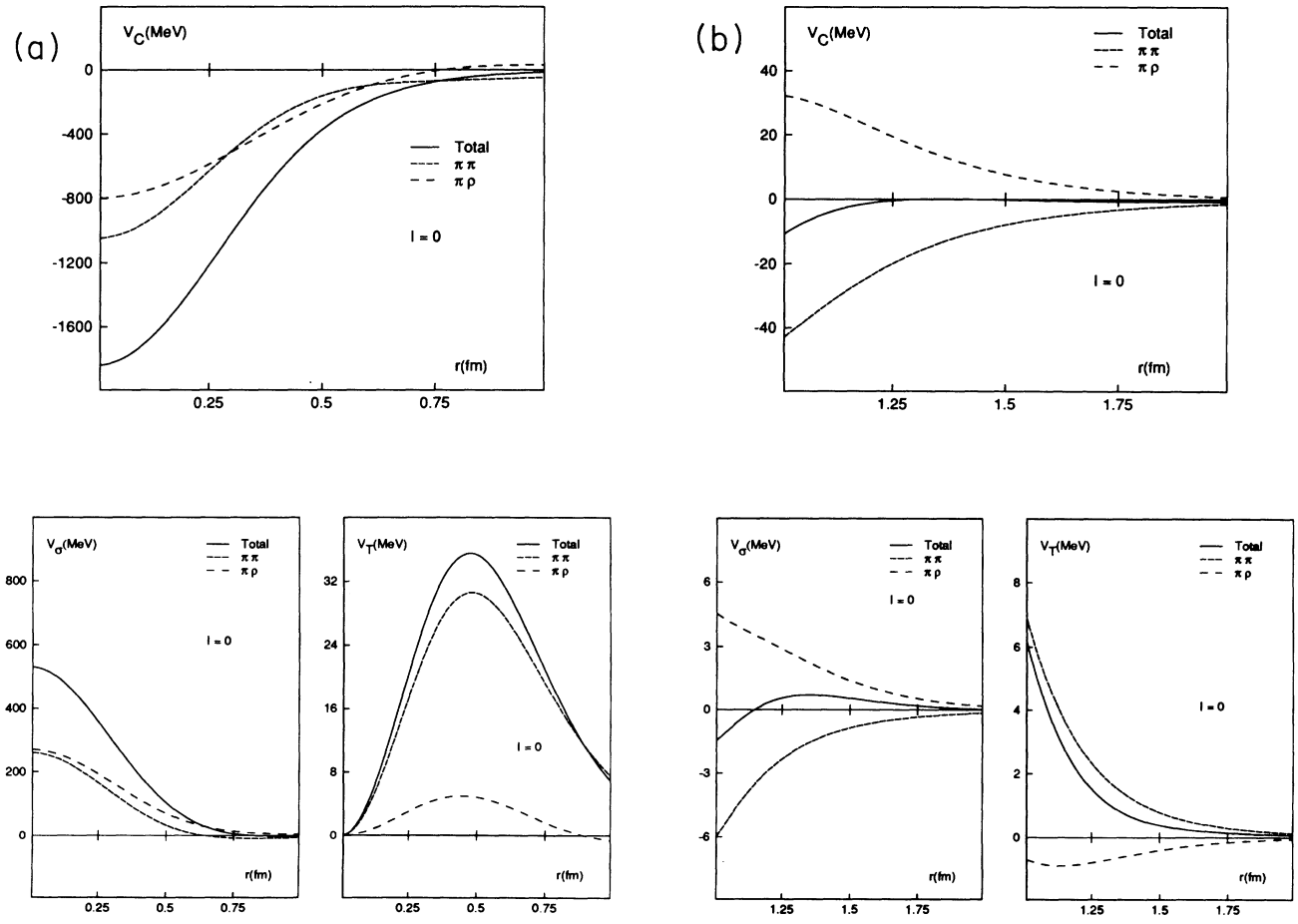

FIG. 10. Central, spin-spin, and tensor $\pi\pi$- and $\pi\rho$-exchange potentials with $N\Delta$ and $\Delta\Delta$ intermediate states. The total contribution is also shown. (a) $I = 0$ and $r \leq 1$ fm; (b) $I = 0$ and $1 \leq r \leq 2$ fm; (c) $I = 1$ and $r \leq 1$ fm; (d) $I = 1$ and $1 \leq r \leq 2$ fm.

$$u^{\mu}(p,\sigma) = \left(\frac{E+M_{\Delta}}{2M_{\Delta}}\right)^{1/2} L^{(1)}(p)^{\mu}_{\nu} \left(\frac{1}{E+M_{\Delta}}\right) \Sigma^{\dagger\nu}_{N\Delta}\psi_{\sigma}. \tag{A6}$$

The spin-1 boost gives

$$L^{(1)}(p)^{\mu}_{\nu}\ \Sigma^{\dagger\nu}_{N\Delta} = \left(\frac{1}{M_{\Delta}}\mathbf{p}\cdot\boldsymbol{\Sigma}^{\dagger}, \boldsymbol{\Sigma}^{\dagger}\right) \approx \left(0, \boldsymbol{\Sigma}^{\dagger}\right) . \tag{A7}$$

This last approximation is used in our potential calculations.

APPENDIX B: DIFFERENTIATION DICTIONARY

In this Appendix we give a dictionary for the evaluation of the differentiations in Eqs. (4.7), (4.13), (4.16), and (4.18). The procedure is described in more detail in Appendix B of Ref. [2].

(1) For $O^{(\alpha)}_{N\Delta}(\boldsymbol{\nabla}_1, \boldsymbol{\nabla}_2)$:

$$\text{(1a)}\ \lim_{\mathbf{r}_1\to\mathbf{r}_2} (\boldsymbol{\sigma}_1\cdot\boldsymbol{\nabla}_1)(\boldsymbol{\sigma}_2\cdot\boldsymbol{\nabla}_2)\boldsymbol{\nabla}_2^2\ F(r_1)G(r_2) = \frac{1}{3}F'(r)\left[-\frac{2}{r^2}G'(r) + \frac{2}{r}G''(r) + G'''(r)\right]((\boldsymbol{\sigma}_1\cdot\boldsymbol{\sigma}_2) + S_{12}) ,$$

$$\begin{aligned}\text{(1b)}\ \lim_{\mathbf{r}_1\to\mathbf{r}_2} &(\boldsymbol{\nabla}_1\cdot\boldsymbol{\nabla}_2)(\boldsymbol{\sigma}_1\cdot\boldsymbol{\nabla}_2)(\boldsymbol{\sigma}_2\cdot\boldsymbol{\nabla}_2)\ F(r_1)G(r_2) \\ &= \frac{1}{3}F'(r)\left[-\frac{2}{r^2}G'(r) + \frac{2}{r}G''(r) + G'''(r)\right](\boldsymbol{\sigma}_1\cdot\boldsymbol{\sigma}_2) \\ &\quad + \frac{1}{3}F'(r)\left[\frac{1}{r^2}G'(r) - \frac{1}{r}G''(r) + G'''(r)\right]S_{12} ,\end{aligned}$$

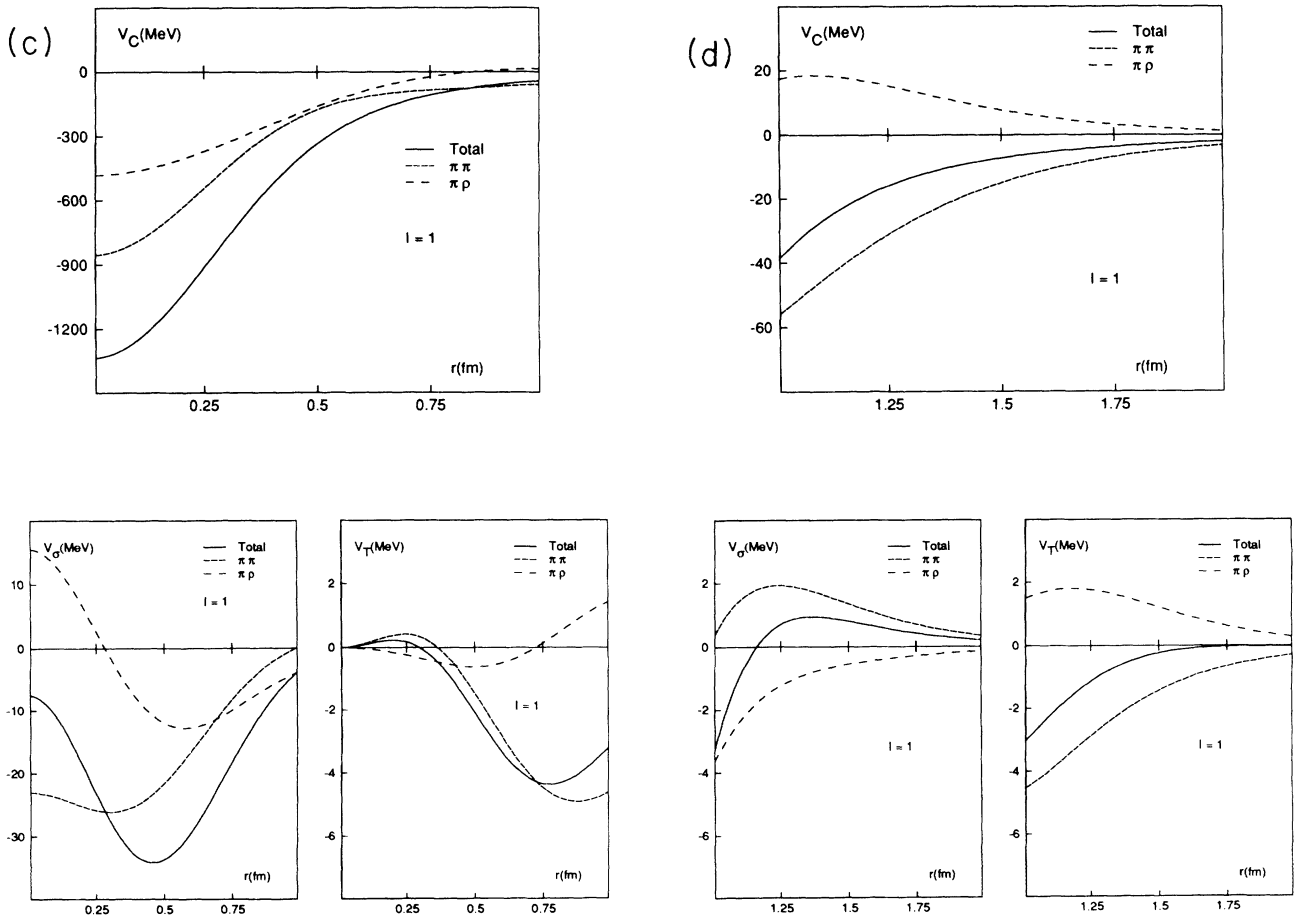

FIG. 10. (*Continued*).

(1c) $\lim_{\mathbf{r}_1\to\mathbf{r}_2}(\boldsymbol{\sigma}_1\cdot\boldsymbol{\nabla}_1)(\boldsymbol{\sigma}_2\cdot\boldsymbol{\nabla}_2)(\boldsymbol{\sigma}_2\cdot\boldsymbol{\nabla}_1\times\boldsymbol{\nabla}_2)\ F(r_1)G(r_2)$

$$= \frac{2i}{3}\left[\frac{1}{r}F'(r)G''(r)+\frac{1}{r}F''(r)G'(r)+\frac{1}{r^2}F'(r)G'(r)\right](\boldsymbol{\sigma}_1\cdot\boldsymbol{\sigma}_2)$$
$$+\frac{i}{3}\left[\frac{1}{r}F'(r)\left(\frac{1}{r}G'(r)-G''(r)\right)-\left(\frac{1}{r}F'(r)-F''(r)\right)\frac{2}{r}G'(r)\right]S_{12}\ ,$$

(1d) $\lim_{\mathbf{r}_1\to\mathbf{r}_2}(\boldsymbol{\nabla}_1\cdot\boldsymbol{\nabla}_2)(\boldsymbol{\sigma}_2\cdot\boldsymbol{\nabla}_2)(\boldsymbol{\sigma}_2\cdot\boldsymbol{\sigma}_1\times\boldsymbol{\nabla}_1)\ F(r_1)G(r_2)$

$$= \frac{2i}{3}\left[F''(r)G''(r)+\frac{2}{r^2}F'(r)G'(r)\right](\boldsymbol{\sigma}_1\cdot\boldsymbol{\sigma}_2)-\frac{i}{3}\left[F''(r)G''(r)-\frac{1}{r^2}F'(r)G'(r)\right]S_{12}\ ,$$

(1e) $\lim_{\mathbf{r}_1\to\mathbf{r}_2}(\boldsymbol{\sigma}_2\cdot\boldsymbol{\nabla}_2)(\boldsymbol{\sigma}_2\times\boldsymbol{\nabla}_1\cdot\boldsymbol{\nabla}_1\times\boldsymbol{\nabla}_2)\ F(r_1)G(r_2)$

$$= -\frac{2}{r}\left[\frac{1}{r}F'(r)G'(r)+F'(r)G''(r)+F''(r)G'(r)\right]\ .$$

(2) For $O^{(\alpha)}_{\Delta\Delta}(\boldsymbol{\nabla}_1,\boldsymbol{\nabla}_2)$:

(2a) $\lim_{\mathbf{r}_1\to\mathbf{r}_2}(\boldsymbol{\nabla}_1\cdot\boldsymbol{\nabla}_2)^2\ F(r_1)G(r_2) = \frac{2}{r^2}F'(r)G'(r)+F''(r)G''(r)\ ,$

(2b) $\lim_{\mathbf{r}_1\to\mathbf{r}_2}(\boldsymbol{\nabla}_1\cdot\boldsymbol{\nabla}_2)(\boldsymbol{\sigma}_1\cdot\boldsymbol{\nabla}_2)(\boldsymbol{\sigma}_2\cdot\boldsymbol{\nabla}_1)\ F(r_1)G(r_2)$

$$= \frac{1}{3}\left[\frac{2}{r^2}F'(r)G'(r)+F''(r)G''(r)\right](\boldsymbol{\sigma}_1\cdot\boldsymbol{\sigma}_2)$$
$$+\frac{1}{3}\left[-\frac{1}{r^2}F'(r)G'(r)+F''(r)G''(r)\right]S_{12}\ ,$$

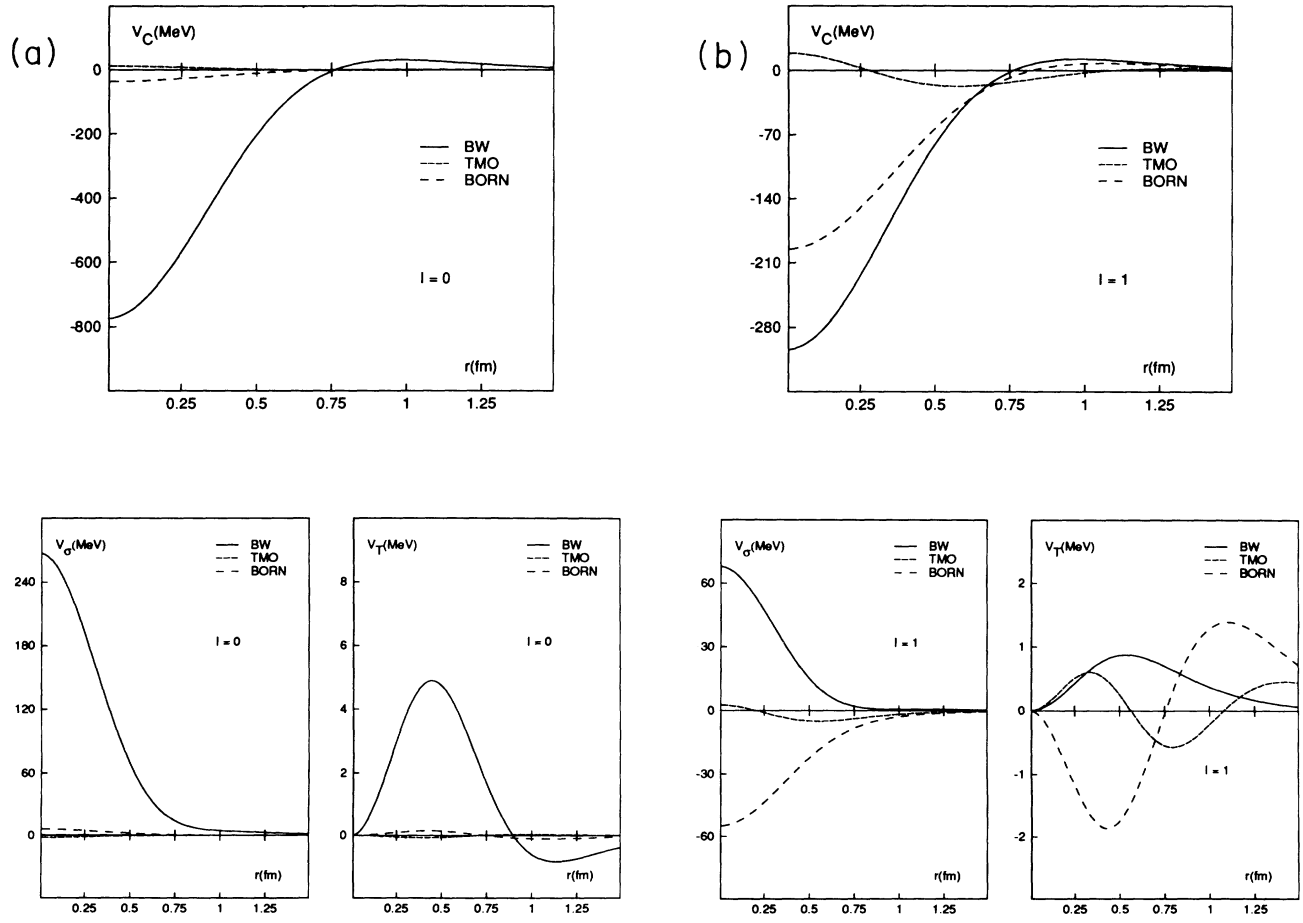

FIG. 11. Isobar $\pi\rho$-exchange contributions of the BW, TMO, and Born diagrams for (a) $I = 0$ and (b) $I = 1$.

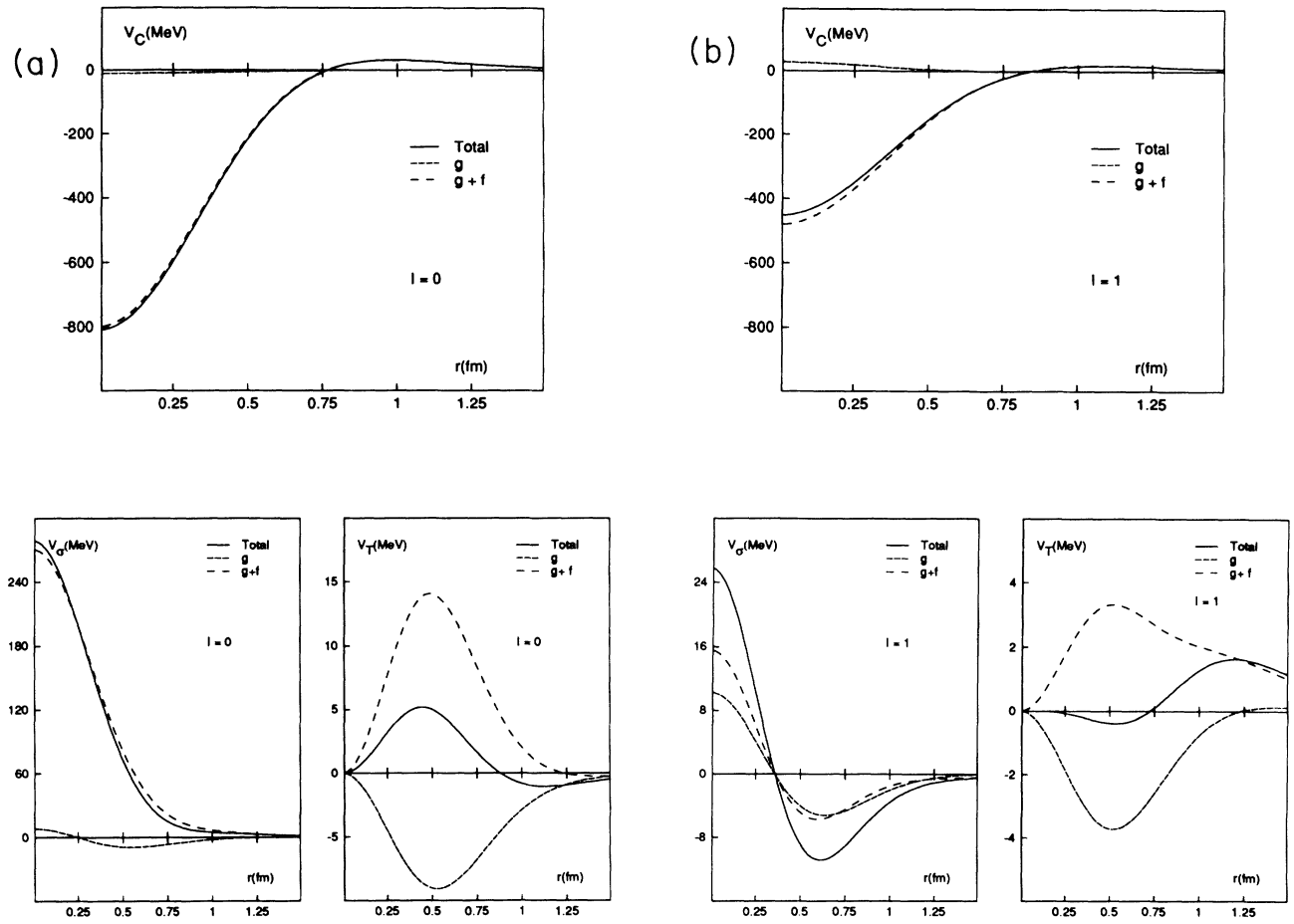

FIG. 12. Electric g and magnetic $(g+f)$ contributions of the isobar $\pi\rho$-exchange potential for (a) $I=0$ and (b) $I=1$. The electric and magnetic parts correspond to those of Eq. (4.7).

$$\text{(2c)}\ \lim_{\mathbf{r}_1\to\mathbf{r}_2}(\boldsymbol{\sigma}_1\cdot\boldsymbol{\nabla}_1)(\boldsymbol{\sigma}_2\cdot\boldsymbol{\nabla}_1)\boldsymbol{\nabla}_2^2\,F(r_1)G(r_2)=\frac{1}{3}\left[\Delta F(r)(\boldsymbol{\sigma}_1\cdot\boldsymbol{\sigma}_2)-\left(\frac{1}{r}F'(r)-F''(r)\right)S_{12}\right]\Delta G(r)\ ,$$

$$\text{(2d)}\ \lim_{\mathbf{r}_1\to\mathbf{r}_2}(\boldsymbol{\nabla}_1\times\boldsymbol{\nabla}_2)^2\,F(r_1)G(r_2)=\frac{2}{r}\left[\frac{1}{r}F'(r)G'(r)+(F'G')'(r)\right]\ ,$$

$$\text{(2e)}\ \lim_{\mathbf{r}_1\to\mathbf{r}_2}(\boldsymbol{\nabla}_1\cdot\boldsymbol{\nabla}_2)(\boldsymbol{\nabla}_1\times\boldsymbol{\nabla}_2)\,F(r_1)G(r_2)=0\ ,$$

where Δ is the Laplacian:

$$\Delta G(r)=G''(r)+\frac{2}{r}G'(r)\ .$$

[1] Th.A. Rijken, Ann. Phys. (N.Y.) **208**, 253 (1991).
[2] Th.A. Rijken and V.G.J. Stoks, Phys. Rev. C **46**, 73 (1992), the preceding paper.
[3] J.W. Durso, M. Saarela, G.E. Brown, and A.D. Jackson, Nucl. Phys. **A278**, 445 (1977).
[4] K. Holinde, R. Machleidt, M.R. Anastasio, A. Faessler, and H. Müther, Phys. Rev. C **18**, 870 (1978); *ibid.* **24**, 1159 (1981); X. Bagnoud, K. Holinde, and R. Machleidt, *ibid.* **29**, 1792 (1984).
[5] P. Haapakoski, Phys. Lett. **48B**, 307 (1974); A.M. Green, Rep. Prog. Phys. **39**, 1109 (1976).
[6] M. Chemtob, J.W. Durso, and D.O. Riska, Nucl. Phys. **B38**, 141 (1972).
[7] K.A. Brueckner and K.M. Watson, Phys. Rev. **92**, 1023 (1953), hereafter referred to as BW.
[8] M. Taketani, S. Machida, and S. Ohnuma, Prog. Theor. Phys. (Kyoto) **7**, 45 (1952), hereafter referred to as TMO.
[9] Th.A. Rijken and V.G.J. Stoks (unpublished).

[10] We follow the conventions of J.D. Bjorken and S.D. Drell, *Relativistic Quantum Mechanics* and *Relativistic Quantum Fields* (McGraw-Hill, New York, 1965).
[11] M.M. Nagels, T.A. Rijken, and J.J. de Swart, Phys. Rev. D **17**, 768 (1978).
[12] P.M.M. Maessen, T.A. Rijken, and J.J. de Swart, Phys. Rev. C **40**, 2226 (1989).
[13] R. Machleidt, K. Holinde, and Ch. Elster, Phys. Rep. **149**, 1 (1987).
[14] T.A. Rijken, Ph. D. thesis, University of Nijmegen, 1975.
[15] J.R. Bergervoet, P.C. van Campen, R.A.M. Klomp, J.-L. de Kok, T.A. Rijken, V.G.J. Stoks, and J.J. de Swart, Phys. Rev. C **41**, 1435 (1990).
[16] H.J. Weber and H. Arenhövel, Phys. Rep. C **36**, 277 (1978).
[17] P.R. Auvil and J.J. Brehm, Phys. Rev. **145**, 1152 (1966).